Available online at www.sciencedirect.com

jmr&t Journal of Materials Research and Technology

www.jmrt.com.br

Original Article

A new insight into the temperature induced molecular aggregations in tris(8-hydroxyquinoline) metals

Fahmi F. Muhammadsharif[a,*], *Suhairul Hashim*[b,c,*], *Khaulah Sulaiman*[d], *G. Baldacchini*[e]

[a] *Department of Physics, Faculty of Science and Health, Koya University, 44023 Koya, Kurdistan Region-F.R., Iraq*
[b] *Department of Physics, Faculty of Science, Universiti Teknologi Malaysia (UTM), 81310 Skudai, Johor, Malaysia*
[c] *Centre for Sustainable Nanomaterials (CSNano), Ibnu Sina Institute for Scientific and Industrial Research (ISI-SIR), Universiti Teknologi Malaysia (UTM), 81310 Skudai, Johor, Malaysia*
[d] *Low Dimensional Materials Research Centre, Department of Physics, Faculty of Science, University of Malaya, 50603 Kuala Lumpur, Malaysia*
[e] *Via Guglielmo Quattrucci 246, Grottaferrata, 00046 Rome, Italy, formerly ENEA, Frascati Research Center, 00044 Frascati, Rome, Italy*

ARTICLE INFO

Article history:
Received 25 December 2019
Accepted 22 February 2020
Available online 6 March 2020

Keywords:
Tris(8-hydroxyquinoline) metal
Gaq_3
Molecular aggregation
Polyamorphism
PL blueshift

ABSTRACT

Annealing of tris(8-hydroxyquinoline) gallium (Gaq_3) film at various temperatures in dry N_2 atmosphere has shown the existences of four different phases of molecular aggregations before the burning out of the film at about 310 °C. The first three phases, up to 235 °C, are amorphous molecular aggregations, while the fourth one at 255 °C is a crystalline structure, very likely α-polymorph. The photoluminescence (PL) intensity was increased to about five times greater than that of the pristine film at 235 °C, while the PL peak was blue shifted consistently. Although a small contribution of Rayleigh scattering cannot be excluded at high temperatures when crystallites appear, the PL blueshift was mainly attributed to the nanostructured molecular aggregations followed by enhanced PL intensity. These new findings can be a common characteristic of organometallic complexes at varied annealing temperatures. The presented results open a new route of fabricating highly emissive thin films of amorphous nanostructure, which are specifically important for organic light emitting diode (OLED) based displays.

1. Introduction

Over the past decade, research progress in organic materials has led to great achievements in the development of nano-photonics and nano-electronic devices [1,2]. This is mainly due to the excellent chemical and physical properties offered by these kinds of materials including easy molecular designability, optical and electronics tunability [3–8]. One of the most practical achievements is related to the technological advancement of organic light emitting diode (OLED) thanks to the unique emissive behavior of organometal-

* *Corresponding authors.*
E-mails: fahmi.fariq@koyauniversity.org (F.F. Muhammadsharif), suhairul@utm.my (S. Hashim).
https://doi.org/10.1016/j.jmrt.2020.02.084

lic complexes used as emitting layer of the devices [9–12]. The organometallic complexes offer important optical and electronic properties arising from the interplay between the inorganic materials and the organic ligands. The combination of metals with organic molecules seems to offer possible solutions to many problems in metal extraction and purification [13], in formulation of heat-resistant polymers [14], enhanced photocatalytic performance [15], asymmetric supercapacitors [16–18], surface coatings and chemical synthesis [19–21]. Tris(8-hydroxyquinoline) metals, Mq_3 (M = Ga and Al), are the most widely studied organometallics for their interesting optoelectronics properties [22–24], photonic response selectivity and thermal stability [25,26]. The use of Alq_3 and Gaq_3 has also been extended for the application of organic solar cells (OSCs) as buffer/hole blocking layer between the active layer and aluminum electrode [27], and as a dopant molecular acceptor in the active layer of solution-processed OSCs [28,29]. It has been found in these studies that the contribution of Gaq_3 and Alq_3 is to improve the overall performance, reproducibility and stability of OSCs.

It is obvious that intrinsic and extrinsic characteristics of organic materials are playing a vital role in the performance selectivity of organic electronics devices. In these contexts, various approaches have been reported to modify the nanoscale properties of organic materials for desired applications [30–32]. Although these changes are responsible to the enhancement of the device's performance, there is yet a lack of complete understanding and reasoning for such improvements. That is because the operation of electronic devices is highly dependent on the nanoscale behavior, size and architecture of their active organic components [33–37], which is not an easy task to be fully addressed due to both instrumental limitations and sophisticated phenomena at the low dimensional scales.

The morphology of organic films are highly affected by the nature of molecular aggregations due to weak interactions between adjacent molecules, such as π–π interaction, Van der Waals forces and hydrogen bonding [38]. The resultant forces define the packing pattern of the molecules and hence the shaping of their final periodicity in terms of structural distribution [39,40]. Hence, efforts on modifying/tuning molecular aggregations are of great importance for desired applications, especially when different nanostructures are in concern [41–45]. Nanostructured sizes and shapes are capable of providing enhanced charge carriers mobility in a specific direction, which is quite interesting for the application of single-crystalline based devices [46–48]. Xu et al. produced crystalline Alq3 sub-microwires have by a one-step anti-solvent (the solvent with poor solubility to the solute) diffusion method combined solvent-evaporation-induced self-assembly without surfactant assistant [49], whereas Boulet et al. used a combination of evaporative and antisolvent crystallization to generate vertically-oriented hexagonal prism arrays of Alq3, and vertical half-disks and sharp-edged rectangular prisms of Znq2 [50]. Besides, Gu et al. reported that through a suitable combination of solvent and anti-solvent with controllable surface tension difference, the droplets can automatically cracked into the micro-droplets, which provides an aggregation force directing toward the center of the droplet to drive the low-dimensional building blocks to form the special aggregations during the self-assembly process [51]. The concept of antisolvent approach was also realized Yin et al. to achieve a sequential epitaxial growth to synthesize dual-color-emitting organic heterostructures with 9,10-bis(phenylethynyl) anthracene (BPEA) microwire trunks and Alq3 microstructure branches [52].

In recent years, investigations on photoluminescence (PL) intensity of Alq_3 and its structural related consequences have become the subject of a lively debate, whereby different explanations for PL blueshift were proposed [53–55]. On one hand, the PL blueshift has been ascribed to the roleplay between meridianal and facial isomers [56,57], and on the other hand to the intermolecular interactions of the meridianal isomer alone [55]. PL blueshift in Alq_3 was wrongly attributed to the Rayleigh scattering phenomenon [58,59], and this explanation appeared rather vague in Gaq_3, where it has been noticed that the energy gap of non-crystalline Gaq3 film is red shifted, while its PL is blue shifted [26]. Hence, it was concluded that intermolecular interactions and molecular rearrangements are responsible for the observed blueshift [26,53]. Baldacchini et al. [60] claimed the existence of four different components of molecular aggregation, because the PL of Alq_3 films decays in air with four different amplitudes and constant times, which has led to formulize the Four Components Model (FCM). In an extended approach, the stretched FCM model, was able to fit the PL of Alq_3 molecules during a decay of six years in Air, and an interpretation of the physical phenomena has been given by introducing a 0th-order kinetics [53].

It is commonly held that structure and morphology of Mq_3 films play a crucial role in defining their PL behavior, hence any systematic study addressing correlation between PL and molecular aggregations is of special importance. Moreover, PL quenching and degradation processes have been often ascribed to the formation of crystallites, migration of ionic and molecular species, and chemical reactions, but none of them have been quantified in a simple and reproducible way [61–63]. We have previously showed that meridianal α-polymorph can be grown within the amorphous phase of Gaq_3 films with increasing temperature, and hence contributing to a PL blueshift [64]. However, the weakly onset of a Gaq_3 polymorphism at high temperatures has introduced a dubious debate, because of the opposite shifting of PL and energy gap.

In the current research work, an exclusive attention is devoted to any possible correlation between molecular aggregations and PL position or PL intensity in Gaq_3 films. For this purpose, morphological growth states and PL profile of Gaq_3 films have been specifically investigated at temperatures from 85 to 255 °C in dry N_2 gas. The contribution of this study is to understand how molecular aggregations, either to be polymorphism or polyamorphism, contribute to the PL blueshift and luminescence variation in Gaq_3, and in Mq_3 films. The remainder of the paper is organized as follows: the methodology of the film formation and temperature induced morphological modifications are presented in section 2, followed by analysis and discussion of the obtained results in section 3. Finally, the main conclusions are given in section 4.

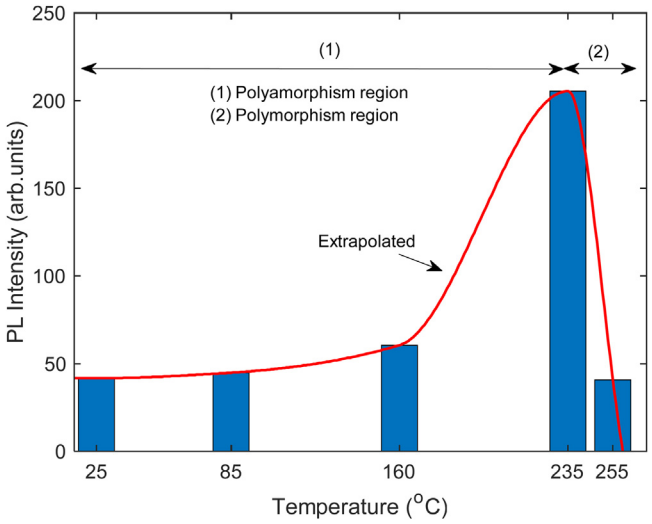

Fig. 1 – PL intensity of Gaq_3 film with increased annealing temperature.

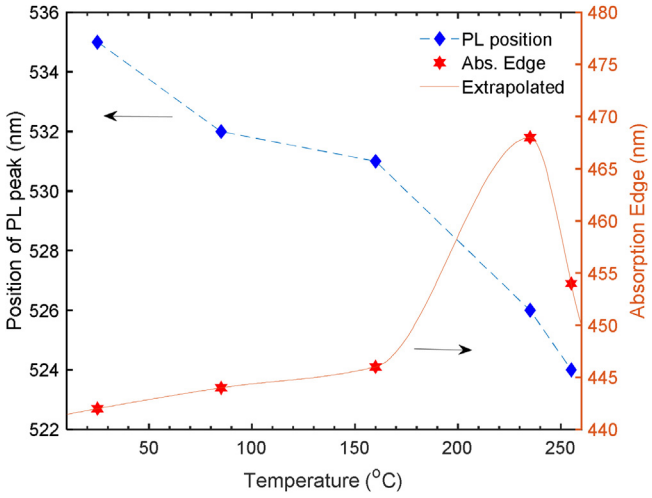

Fig. 2 – Wavelength position of PL peak and absorption edge of Gaq_3 film with increased annealing temperature.

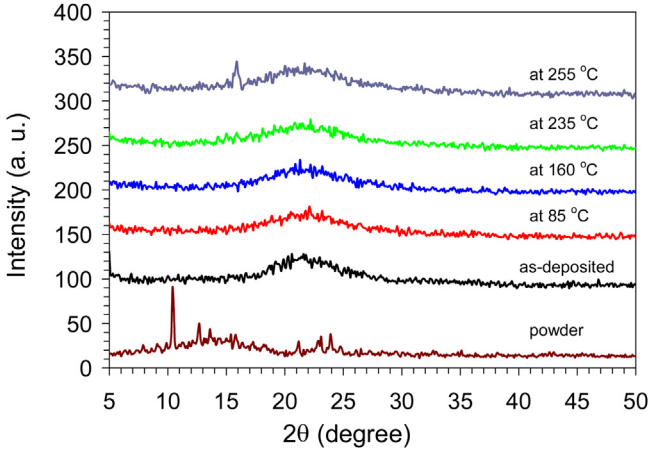

Fig. 3 – XRD patterns for the pristine and annealed Gaq_3 films under N_2 gas.

2. Materials and methods

Tris(8-hydroxyquinolinate) gallium (Gaq_3), $Ga(C_9H_6NO)_3$, was purchased from Sigma–Aldrich in powder form and used as received without further purification. Precleaned quartz substrates were used at room temperature (RT) to deposit Gaq_3 films onto them via a homemade thermal evaporator under a pressure of about 10^{-4} mbar. The quartz substrates were cleaned with Decon® Neutracon foam for 15 min in ultrasonic bath. Later on, they were rinsed and sonicated with acetone, ethanol and distilled water sequentially for 10 min. Lastly, the quartz substrates were dried thoroughly by nitrogen gas. Thickness of the deposited Gaq_3 films was measured by a KLA Tensor P-6 surface profilometer. The films were post annealed within a barrel furnace under dry nitrogen gas for 10 min. The annealing temperatures were set at 85, 160, 235, and 255 °C. The PL spectra were measured with a LS50B PERKIN ELMER luminescence spectrometer in the wavelength range from 200 to 800 nm at the excitation wavelength of 396 nm. X-ray diffractometer (Bruker AXS) was applied to record the XRD patterns using Cu K_α radiation of wavelength λ = 1.5406 A° as a source. Field emission scanning electronic microscopy, FESEM (Quanta 200 F), was utilized to capture the morphology of the films before and after annealing processes. The photo absorption properties of the films were assessed by a Jasco V-570 UV–VIS–NIR spectrophotometer.

3. Results and discussion

The strength of PL emission of Gaq_3 films at increased annealing temperatures is reported in Fig. 1; an extrapolated red line joins the peak values smoothly in order to better observe the trend of the changes. The presence of a unique PL peak, which reaches a maximum of five times higher than that of the pristine film, at temperature of 235 °C, could be a consequence of the structural and thickness variations of the films. Indeed, it has been reported that PL intensity depends on the isomeric type and structure of the film [25,54]. It was observed that PL intensity is increased with the film thickness [65], and it is quenched with increasing crystallinity [26,66].

In our films, the impact of thickness is ruled out for two reasons. First, a notable shrink in the energy gap of the films, due to enhanced overlap of compact molecules and denser π–π stacking [58,65], was found by increasing temperature [26]. Hence, an opposite trend of decreasing PL intensity, due to denser film, should have been observed along the entire temperature range, which is not the case (see Fig. 1). Second, the absorption edge of the energy gap and the wavelength position of the PL peak was seen to be changed in opposite manner when annealing temperature was increased, as shown in Fig. 2. Therefore, the consistent increase of PL emission in Fig. 1, and noteworthy blueshift of the PL peak in Fig. 2, can be very likely attributed to the morphological changes or molecular aggregations of the Gaq_3.

We noticed that α-polymorph can be produced from the amorphous phase of meridianal Gaq_3 upon rising temperature, leading to a quenched luminescence and PL blueshift [64].

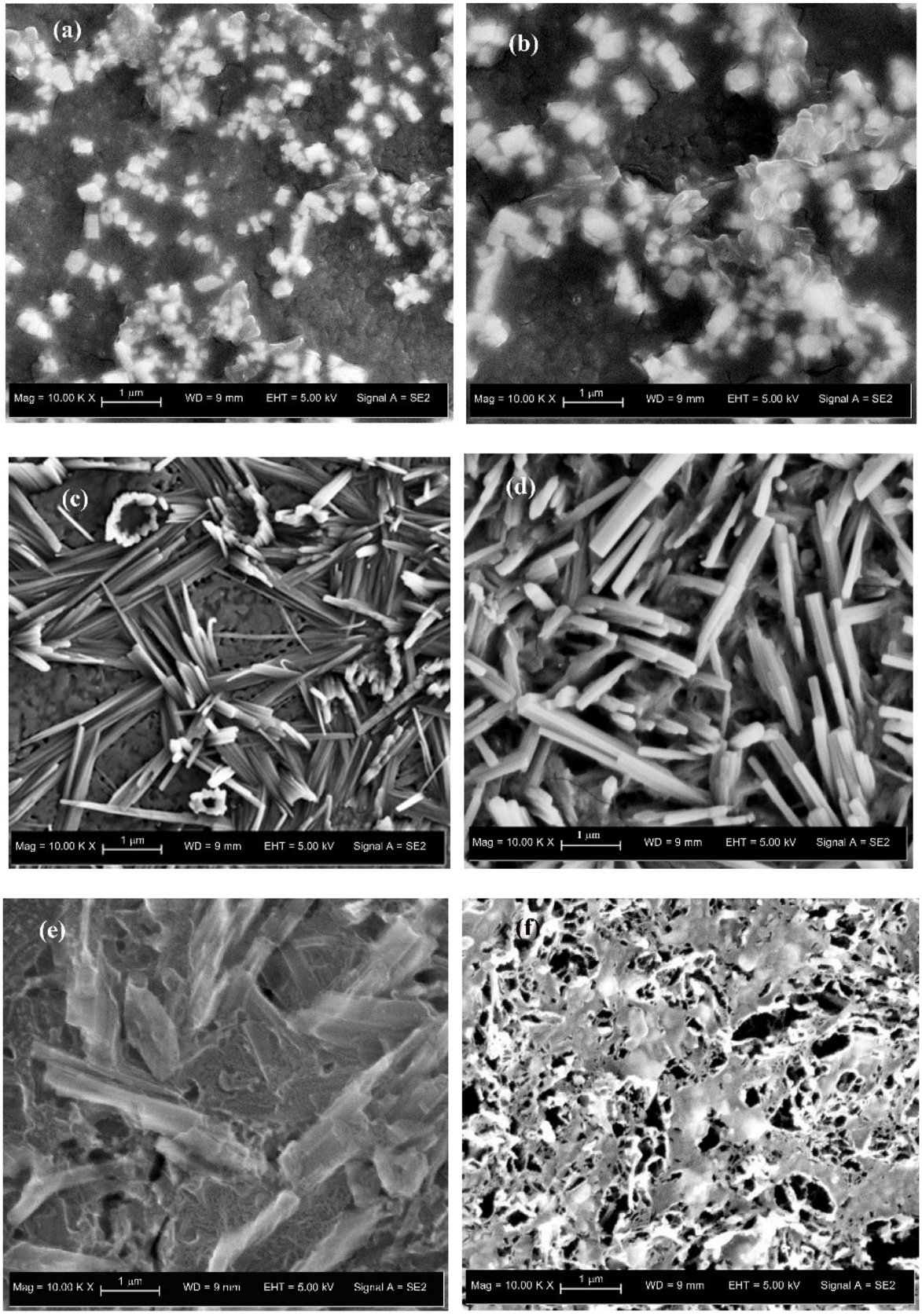

Fig. 4 – Molecular aggregation images of Gaq_3 films at RT (a), 85 °C (b), 160 °C (c), 235 °C (d), 255 °C (e) and 310 °C (f), captured by FESEM technique.

Meanwhile, it was observed from the XRD measurements (see Fig. 3) that this polymorphism occurs weakly at 255 °C, that is beyond the glass transition temperature (T_g) [26]. Because of these findings and that Gaq_3 films are yet in the amorphous phase, the steady rise of PL emission and its continuous blueshift, from room temperature (RT) to 235 °C, require a new interpretation for the contribution of amorphous states (we call it here polyamorphism) to these optical changes. Therefore, the attribution of the PL blueshift to Rayleigh scattering alone [58,59] should be considered as untenable explanation.

PL blueshift has been already ascribed to the intermolecular interactions of the meridianal isomer [55], whereas molecular rearrangements can play a vital role in this shift [26]. Although morphological changes of Alq_3 at different temperatures have not yet accurately measured, Baldacchini et al. [53] reported the existence of four different components of molecular aggregations, claiming that the PL of Alq_3 films decays in air following four different pathways. To clarify the previous lacking of structural and morphological states, we have specifically taken into consideration the deep surface images of Gaq_3 films at different temperatures, as shown in Fig. 4. Upon a close look at the surface of the Gaq_3 films, it is clear that temperature has produced pronounced modifications in the molecular aggregations. In particular, four different phases of molecular aggregation/rearrangement have been observed. In the first phase, from RT to about 160 °C, Fig. 4(a) and (b), there exist bunches of molecular aggregation, while at 160 °C, Fig. 4(c), the second phase of molecular aggregation is observed in the form of a grown grass. Increasing the temperature to about 235 °C led to the formation of a third phase in the form of nanorod aggregation, Fig. 4(d), while the laminated form of molecular aggregation at 255 °C can be considered as the fourth phase that was resulted from degradation of the nanorods due to hard heating, as shown in Fig. 4(e). Noteworthy, at the high enough temperature of about 310 °C, the film burned out with clear dark spots left on the surface of the substrate, as shown in Fig. 4(f).

Because of the structural changes in the films, the crystallites were formed only at 255 °C. Therefore, the first three phases of the molecular aggregations are amorphous packings, while crystalline structures are assembled in the fourth phase, very likely α-polymorph. In conclusion, polyamorphism seems to be the main factor affecting luminescence enhancement and its blueshift in the organometallic complexes, such as Alq_3, Gaq_3, and Inq_3. In the present case, meridianal Gaq_3 films under flowing N_2 gas at atmospheric pressure are stable in different amorphous phases from RT to about 235 °C. It is worth noting that the onset of meridianal α-polymorph at 255 °C is a further evidence of the difficulties, if not impossibility, to activate thermally the isomeric transition from meridianal to facial in Gaq_3 films, which is in agreement with the results obtained in Alq_3 films deposited by thermal evaporation [55].

When higher density Gaq_3 nanorods was formed, larger PL intensity was observed on the emission spectra, as in Fig. 1. This result is similar to that obtained for α-polymorph Alq_3 nanowires grown under Ar gas at appropriate pressure [67], except that in our films complete amorphous nanorods were formed. However, crystalline Gaq_3 in the form of one-dimensional nanostructure and nanosphere, fabricated by thermal evaporation under cold trap in the presence of pressurized He or Ar gas, showed similar PL intensity [68]. These differences in the formation of various nanostructures and their optical properties might be ascribed to the effects of gases and pressures utilized during the grown process [25,69]. Anyway, it seems well ascertained that PL intensity of amorphous nanostructures is always higher than that of their crystalline counterparts. Indeed, this feature could be a consequence of excited charge carriers in crystalline regions moving at longer distances before their recombination or relapsing, leading to an increased non-radiative probability.

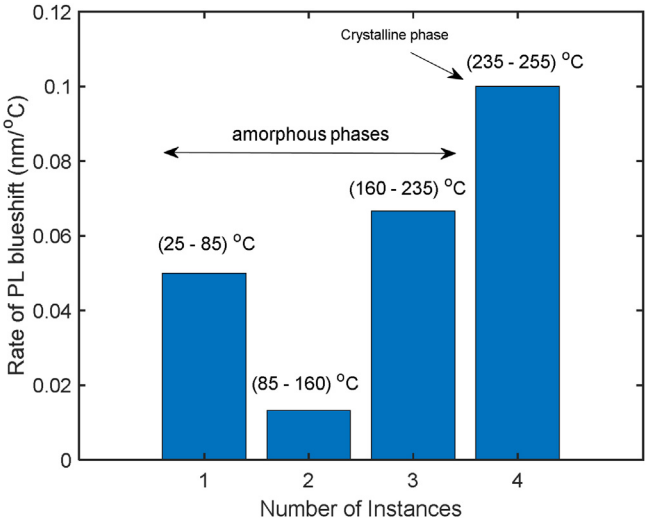

Fig. 5 – The rate of PL blueshift of Gaq_3 films with temperature.

Now, considering the rate of PL blueshift with temperature, as shown in Fig. 5, it is observed that the crystalline α-polymorph produced the highest PL blueshift, followed by the third amorphous phase in which the nanostructures possess the highest density. It is concluded that the nanostructured amorphous phases (polyamorphism) is highly contributed to the PL blueshift, which adds on the importance of such molecular aggregations on PL intensity and its blueshift in these organometallic complexes. Nevertheless, a small contribution may also derive by the Rayleigh scattering in the crystalline phase, although such phenomenon was excluded in Alq_3 [49]. More detailed information can be obtained on isomeric transitions and their phases, only by performing new systematic experiments at more annealing temperatures and gases.

4. Conclusions

A careful study on Gaq_3, in particular its PL and blueshift at different annealing temperatures under dry N_2 gas was performed. It has been observed at 235 °C that the PL intensity increased five times with respect to the pristine film, and at the same time, a PL blueshift is emerging in a consistent way as temperature increases. Moreover, four different phases of molecular aggregations have been observed by means of field emission microscopy. Of them, the first three are polyamorph

bunches, while the fourth one appears at 255 °C, and very likely is a crystalline α-polymorph. These crystallites produced the highest blueshift, soon followed by the third amorphous phase that possesses the highest density. However, x-rays diffraction has shown that the amount of crystalline aggregations is very low in the annealed films at 255 °C, so that their contribution to the Rayleigh scattering is scarcely significant, if any. On the contrary, a continuous blueshift is produced by the three amorphous phases from RT to 235 °C, which are composed of meridianal isomers and are the bulk of films. It can be concluded that nanostructured molecular aggregation is the main reason affecting PL and blueshift in particular and the optical properties of organometallic complexes in general.

Conflict of interest

The authors declare no conflicts of interest.

Data availability

The raw/processed data required to reproduce these findings are presented in the manuscript.

Acknowledgment

The authors acknowledge University of Malaya for the research facility support received from grant RP007A/13AFR. We aslo acknowledge Universiti Teknologi Malaysia for the financial assistance received from vot 07G90 to support the publication fee.

REFERENCES

[1] McAlpine MC, Friedman RS, Jin S, Lin K-h, Wang WU, Lieber CM. High-performance nanowire electronics and photonics on glass and plastic substrates. Nano Lett 2003;3:1531–5.
[2] Sekitani T, Nakajima H, Maeda H, Fukushima T, Aida T, Hata K, et al. Stretchable active-matrix organic light-emitting diode display using printable elastic conductors. Nat Mater 2009;8:494.
[3] Muhammad FF, Sulaiman K. Tuning the optical band gap of DH6T by Alq3 dopant. Sains Malays 2011;40:17–20.
[4] Muhammad FF, Yahya MY, Aziz F, Rasheed MA, Sulaiman K. Tuning the extinction coefficient, refractive index, dielectric constant and optical conductivity of Gaq3 films for the application of OLED displays technology. J Mater Sci Mater Electron 2017;28:14777–86.
[5] Kim M-J, An TK, Kim S-O, Cha H, Kim HN, Xiofeng T, et al. Molecular design and ordering effects of alkoxy aromatic donor in a DPP copolymer on OTFTs and OPVs. Mater Chem Phys 2015;153:63–71.
[6] Omidvar A. Electronic structure tuning and band gap opening of nitrogen and boron doped holey graphene flake: the role of single/dual doping. Mater Chem Phys 2017;202:258–65.
[7] Lim LW, Teh CH, Daik R, Sarih NM, Teridi MAM, Muhammad FF, et al. Synthesis and characterization of 2, 2′-bithiophene end-capped dihexyloxy phenylene pentamer and its application in a solution-processed organic ultraviolet photodetector. RSC Adv 2016;6:61848–59.
[8] Gahungu G, Zhang J. "CH"/N substituted mer-Gaq3 and mer-Alq3 derivatives: an effective approach for the tuning of emitting color. J Phys Chem B 2005;109:17762–7.
[9] Chen D, Su S-J. White organic light-emitting diodes based on organometallic phosphors. In: Organometallics and related molecules for energy conversion. Springer; 2015. p. 285–311.
[10] Dodabalapur A. Organic light emitting diodes. Solid State Commun 1997;102:259–67.
[11] Thompson ME, You Y, Shoustikov A, Sibley S, Burrows PE, Forrest SR. OLEDs doped with phosphorescent compounds. Google Patents; 2001.
[12] Singh D, Nishal V, Bhagwan S, Saini RK, Singh I. Electroluminescent materials: metal complexes of 8-hydroxyquinoline—a review. Mater Des 2018;156:215–28.
[13] Efome JE, Rana D, Matsuura T, Lan CQ. Effects of operating parameters and coexisting ions on the efficiency of heavy metal ions removal by nano-fibrous metal-organic framework membrane filtration process. Sci Total Environ 2019;674:355–62.
[14] Zhang J, Zhang J, Imler GH, Parrish DA, Shreeve JM. Sodium and potassium 3, 5-dinitro-4-hydropyrazolate: three-dimensional metal–organic frameworks as promising super-heat-resistant explosives. Acs Appl Energy Mater 2019;2:7628–34.
[15] Zhang GC, Zhong J, Xu M, Yang Y, Li Y, Fang Z, et al. Ternary BiVO4/NiS/Au nanocomposites with efficient charge separations for enhanced visible light photocatalytic performance. Chem Eng J 2019;375:122093.
[16] Feng M, Gu J, Zhang GC, Xu M, Yu Y, Liu X, et al. Homogeneous nickel bicarbonate nanocrystals as electrode materials for high-performance asymmetric supercapacitors. J Solid State Chem 2020;282:121084.
[17] Chu Y, Zhong J, Fang Z, Yang Y, Qi J, Yu S, et al. Ni (HCO3) 2 nanosheet/nickel tetraphosphate (Ni (P4O11)) nanowire composite as a high-performance electrode material for asymmetric supercapacitors. Nanotechnology 2019;31:015401.
[18] Wang Z, Gu J, Li S, Zhang GC, Zhong J, Fan X, et al. One-step polyoxometalates-assisted synthesis of manganese dioxide for asymmetric supercapacitors with enhanced cycling lifespan. ACS Sustain Chem Eng 2018;7:258–64.
[19] Begum S, Hassan Z, Bräse S, Wöll C, Tsotsalas M. Metal–organic framework-templated biomaterials: recent progress in synthesis, functionalization, and applications. Acc Chem Res 2019;52:1598–610.
[20] Zhang L, Liu H, Shi W, Cheng P. Synthesis strategies and potential applications of metal-organic frameworks for electrode materials for rechargeable lithium ion batteries. Coord Chem Rev 2019;388:293–309.
[21] Zhang W, Wang S, Yang F, Yang Z, Wei H, Yang Y, et al. Synthesis of catalytically active bimetallic nanoparticles within solution-processable metal–organic-framework scaffolds. CrystEngComm 2019;21:3954–60.
[22] Muhammad FF, Hapip AIA, Sulaiman K. Study of optoelectronic energy bands and molecular energy levels of tris (8-hydroxyquinolinate) gallium and aluminum organometallic materials from their spectroscopic and electrochemical analysis. J Organomet Chem 2010;695:2526–31.
[23] Muhammad FF, Sulaiman K. Utilizing a simple and reliable method to investigate the optical functions of small molecular organic films–Alq3 and Gaq3 as examples. Measurement 2011;44:1468–74.
[24] Muhammad FF, Yahya MY, Ketuly KA, Muhammad AJ, Sulaiman K. A study on the spectroscopic, energy band, and optoelectronic properties of α, ω-dihexylsexithiophene/tris (8-hydroxyquinolinate) gallium blends; DH6T/Gaq3

composite system. Spectrochim Acta A Mol Biomol Spectrosc 2016;169:144–51.
[25] Hernández I, Gillin W, Somerton M. Spectroscopic study of Mq3 (M = Al, Ga, In, q= 8-hydroxyquinolinate) at high pressure. J Lumin 2009;129:1835–9.
[26] Muhammad FF, Sulaiman K. Effects of thermal annealing on the optical, spectroscopic, and structural properties of tris (8-hydroxyquinolinate) gallium films grown on quartz substrates. Mater Chem Phys 2011;129:1152–8.
[27] Vivo P, Jukola J, Ojala M, Chukharev V, Lemmetyinen H. Influence of Alq3/Au cathode on stability and efficiency of a layered organic solar cell in air. Sol Energy Mater Sol Cells 2008;92:1416–20.
[28] Muhammad FF, Yahya MY, Sulaiman K. Improving the performance of solution-processed organic solar cells by incorporating small molecule acceptors into a ternary bulk heterojunction based on DH6T: Mq3: PCBM (M = Ga, Al). Mater Chem Phys 2017;188:86–94.
[29] Muhammad FF. Impedance spectroscopy analysis of DH6T: PCBM bulk heterojunction incorporating Gaq3: experiment and model. J Mater Sci Mater Electron 2016;27:637–44.
[30] Kim JS, Park JH, Lee JH, Jo J, Kim D-Y, Cho K. Control of the electrode work function and active layer morphology via surface modification of indium tin oxide for high efficiency organic photovoltaics. Appl Phys Lett 2007;91:112111.
[31] Virkar AA, Mannsfeld S, Bao Z, Stingelin N. Organic semiconductor growth and morphology considerations for organic thin-film transistors. Adv Mater 2010;22:3857–75.
[32] Kango S, Kalia S, Celli A, Njuguna J, Habibi Y, Kumar R. Surface modification of inorganic nanoparticles for development of organic–inorganic nanocomposites—a review. Prog Polym Sci 2013;38:1232–61.
[33] Ma W, Yang C, Gong X, Lee K, Heeger AJ. Thermally stable, efficient polymer solar cells with nanoscale control of the interpenetrating network morphology. Adv Funct Mater 2005;15:1617–22.
[34] Oosterhout SD, Wienk MM, Van Bavel SS, Thiedmann R, Koster LJA, Gilot J, et al. The effect of three-dimensional morphology on the efficiency of hybrid polymer solar cells. Nat Mater 2009;8:818.
[35] Yang SY, Shin K, Park CE. The effect of gate-dielectric surface energy on pentacene morphology and organic field-effect transistor characteristics. Adv Funct Mater 2005;15:1806–14.
[36] Arnold MS, Avouris P, Pan ZW, Wang ZL. Field-effect transistors based on single semiconducting oxide nanobelts. J Phys Chem B 2003;107:659–63.
[37] Muhammad FF, Sulaiman K. Photovoltaic performance of organic solar cells based on DH6T/PCBM thin film active layers. Thin Solid Films 2011;519:5230–3.
[38] Yao W, Han G, Huang F, Chu M, Peng Q, Hu F, et al. “H”-like organic nanowire heterojunctions constructed from cooperative molecular assembly for photonic applications. Adv Sci 2015;2:1500130.
[39] Yan Y, Zhao YS. Organic nanophotonics: from controllable assembly of functional molecules to low-dimensional materials with desired photonic properties. Chem Soc Rev 2014;43:4325–40.
[40] Yao W, Zhao YS. Tailoring the self-assembled structures and photonic properties of organic nanomaterials. Nanoscale 2014;6:3467–73.
[41] Nguyen T-Q, Martel R, Bushey M, Avouris P, Carlsen A, Nuckolls C, et al. Self-assembly of 1-D organic semiconductor nanostructures. J Chem Soc Faraday Trans 2007;9:1515–32.
[42] Burda C, Chen X, Narayanan R, El-Sayed MA. Chemistry and properties of nanocrystals of different shapes. Chem Rev 2005;105:1025–102.
[43] Li R, Hu W, Liu Y, Zhu D. Micro-and nanocrystals of organic semiconductors. Acc Chem Res 2010;43:529–40.
[44] Huang L, Liao Q, Shi Q, Fu H, Ma J, Yao J. Rubrene micro-crystals from solution routes: their crystallography, morphology and optical properties. J Mater Chem 2010;20:159–66.
[45] Xia Y, Yang P, Sun Y, Wu Y, Mayers B, Gates B, et al. One-dimensional nanostructures: synthesis, characterization, and applications. Adv Mater 2003;15:353–89.
[46] Fan C, Zoombelt AP, Jiang H, Fu W, Wu J, Yuan W, et al. Solution-grown organic single-crystalline p-n junctions with ambipolar charge transport. Adv Mater 2013;25:5762–6.
[47] Garcia-Frutos EM. Small organic single-crystalline one-dimensional micro-and nanostructures for miniaturized devices. J Mater Chem C 2013;1:3633–45.
[48] Tang Q, Li H, Liu Y, Hu W. High-performance air-stable n-type transistors with an asymmetrical device configuration based on organic single-crystalline submicrometer/nanometer ribbons. J Am Chem Soc 2006;128:14634–9.
[49] Xu G, Tang Y-B, Tsang C-H, Zapien J-A, Lee C-S, Wong N-B. Facile solution synthesis without surfactant assistant for ultra long Alq3 sub-microwires and their enhanced field emission and waveguide properties. J Mater Chem 2010;20:3006–10.
[50] Boulet J, Mohammadpour A, Shankar K. Insights into the solution crystallization of oriented Alq3 and Znq2 microprisms and nanorods. J Nanosci Nanotechnol 2015;15:6680–9.
[51] Gu J, Yin B, Fu S, Feng M, Zhang Z, Dong H, et al. Surface tension driven aggregation of organic nanowires via lab in a droplet. Nanoscale 2018;10:11006–12.
[52] Yin B, Gu J, Feng M, Zhang GC, Zhang Z, Zhong J, et al. Epitaxial growth of dual-color-emitting organic heterostructures via binary solvent synergism driven sequential crystallization. Nanoscale 2019;11:7111–6.
[53] Baldacchini G, Chiacchiaretta P, Montereali R, Pode R, Vincenti M. Singular photoluminescence behavior of Alq3 films at very long decay time. J Lumin 2018;193:106–13.
[54] Baldacchini G, Chiacchiaretta P, Pode R, Vincenti M, Wang Q-M. Phase transitions in thermally annealed films of Alq3. Low Temp Phys 2012;38:786–91.
[55] Baldacchini G, Chiacchiaretta P, Reisfeld R, Zigansky E. The origin of luminescence blueshifts in Alq3 composites. J Lumin 2009;129:1849–52.
[56] Levichkova M, Assa J, Fröb H, Leo K. Blue luminescent isolated Al q 3 molecules in a solid-state matrix. Appl Phys Lett 2006;88:201912.
[57] Amati M, Lelj F. Luminescent compounds f ac-and m er-aluminum tris (quinolin-8-olate). A pure and hybrid density functional theory and time-dependent density functional theory investigation of their electronic and spectroscopic properties. J Phys Chem A 2003;107: 2560–9.
[58] Higginson KA, Zhang X-M, Papadimitrakopoulos F. Thermal and morphological effects on the hydrolytic stability of aluminum tris (8-hydroxyquinoline)(Alq3). Chem Mater 1998;10:1017–20.
[59] Auzel F, Baldacchini G, Baldacchini T, Chiacchiaretta P, Pode RB. Rayleigh scattering and luminescence blue shift in tris (8-hydroxyquinoline) aluminum films. J Lumin 2006;119:111–5.
[60] Baldacchini G, Baldacchini T, Chiacchiaretta P, Pace A, Pode RB. Photoluminescence and morphology of Alq3 films and four-components model. J Electrochem Soc 2007;154:J217–25.
[61] Aziz H, Popovic ZD. Degradation phenomena in small-molecule organic light-emitting devices. Chem Mater 2004;16:4522–32.
[62] Djurišić A, Lau T, Lam L, Chan W. Influence of atmospheric exposure of tris (8-hydroxyquinoline) aluminum (Alq3): a

photoluminescence and absorption study. Appl Phys A 2004;78:375–80.
[63] Xu M, Xu J. Nanoscale study on origins of the bright clusters in/on moisture-exposed tris (8-hydroxyquinoline) aluminum thin films. Synth Met 2004;145:177–82.
[64] Muhammad FF, Sulaiman K. Optical and morphological modifications in post-thermally treated tris (8-hydroxyquinoline) gallium films deposited on quartz substrates. Mater Chem Phys 2014;148:473–7.
[65] Koay J, Sharif KAM, Rahman SA. Influence of film thickness on the structural, electrical and photoluminescence properties of vacuum deposited Alq (3) thin films on c-silicon substrate. Thin Solid Films 2009;517:5298–300.
[66] Singh R, Kumar J, Singh RK, Kaur A, Sood K, Rastogi R. Effect of thermal annealing on surface morphology and physical properties of poly (3-octylthiophene) films. Polymer 2005;46:9126–32.
[67] Cho C-P, Yu C-Y, Perng T-P. Growth of AlQ3 nanowires directly from amorphous thin film and nanoparticles. Nanotechnology 2006;17:5506.
[68] Yu Y-W, Cho C-P, Perng T-P. Crystalline Gaq 3 nanostructures: preparation, thermal property and spectroscopy characterization. Nanoscale Res Lett 2009;4:820.
[69] Akkuzina A, Kozlova N, Avetisov R, Avetisov IK. The homogeneity range of crystalline tris (8-hydroxyquinoline) gallium. Springer; 2018. p. 85–8. Doklady Chemistry.